Bachelor Project

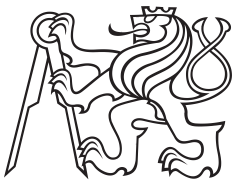

Czech
Technical
University
in Prague

F3

Faculty of Electrical Engineering
Department of Radioelectronics

Long-Distance Digital Troposcatter and Ionoscatter Radio Communication in HF/VHF/UHF band

Jakub Horáček

Supervisor: prof. Ing. Jan Sýkora, CSc.
Field of study: Open Electronic Systems
August 2020

Acknowledgements

I would like to thank the supervisor of this thesis, prof. Ing. Jan Sýkora, CSc., for helping me to find an assignment, that would come up to my expectation. Also I would like to thank people, which were great support during creation of this text.

Declaration

I declare that I completed the presented thesis independently and that all used sources are quoted in accordance with the Methodological instructions that cover the ethical principles for writing an academic thesis.

In Prague, 14. August 2020

Prohlašuji, že jsem předloženou práci vypracoval samostatně, a že jsem uvedl veškerou použitou literaturu.

V Praze, 14. August 2020

Abstract

Aim of this thesis is to get acquainted with fundamentals of radio communications using troposcatter/ionoscatter and summarize these topics. After that we go through available channel models and some advanced methods, which provides better performance for high attenuated scenarios. With this background we firstly implement existing protocol JT9 in Matlab. Although JT9 protocol is itself suitable for high attenuated scenarios, we aim to modify it with obtained knowledge. Experimental long distance link with modified communication protocol need to be setup for verification. At last, we proposed measurement method, that could bring some insight in broadband troposcatter/ionoscatter channel properties.

Keywords: troposcatter, ionoscatter, channel models, LDPC, JT9

Supervisor: prof. Ing. Jan Sýkora, CSc.

Abstrakt

Cílem této práce je seznámit se se základy rádiových komunikací za použití troposférického/ionosférického šíření signálu a shrnout tyto témata. Poté projít dostupné modely přenosových kanálů a některé pokročilé metody, které poskytují lepší výkon pro práci s velmi slabými signály. S tímto za sebou nejprve implementujeme existující protokol JT9 v Matlabu. Ačkoliv je protokol JT9 sám o sobě vhodný pro velmi slabé signály, je naším cílem ho modifikovat za použití získaných znalostí. Pro ověření je nutné provést experimentální dálkové spojení za použití modifikovaného protokolu. Nakonec navrhneme měřící metodu, která by mohla přinést vhled do vlastností přenosového kanálu pro širokopásmové použití troposférického/ionosférického šíření signálu.

Klíčová slova: troposférický přenos, ionosférický přenos, modely přenosového kanálu, LDPC, JT9

Contents

Figures

Tables

Chapter 1

Theoretical background

1.1 Introduction

In a first chapter brief theoretical background about troposcatter/ionoscatter and radio noise is summarized. Then various channel models are introduced along with description od encoding processes for purpose of experimental part. In that is described Matlab implementation of two communication protocols and conducting of experimental links. At the end we discuss possibilities for measurements method for research of troposcatter/ionoscatter channel properties.

1.2 Tropospheric propagation

1.2.1 Troposphere

The troposphere is lowest layer of Earth's atmosphere. Its high differs depending on latitude and season, ranges from 10km to 20km. Lower boundary is Earth's surface, upper is called tropopause and is simply defined as a point where air cease to cool with height. Troposphere physical properties are characterized by temperature, pressure and density, which all significantly varies with altitude, latitude and season. In troposphere occurs all of weather

and short-term variations of atmosphere. Air is here composed of nitrogen (78%), oxygen (21%), argon (0.9%), carbon dioxide (0.03%) ans water vapours (highly variable part).[4] Water vapours may take form of various objects like rain, fog, snow, clouds etc. It's due to physical properties in troposphere. In general are such objects called hydrometeors.[5] [6]

1.2.2 Troposcatter

In troposphere radio signal propagation is subject to several effects. First is refraction, which occurs as a radio wave passes through interface between two layers of atmosphere. These layers emerge as a result of difference in physical properties in parts of atmosphere. Next is attenuation, which is conversion of radio wave energy to thermal energy in attenuating particles which may be gas molecules or hydrometeors. Our main focus is on scattering. It is effect in which radio waves are redirected into various directions and only a part of transmitted energy is in direction to receiver. That leads to significant propagation loss. It can be expressed as

$$P_r = AP_tG_tG_r\left(\frac{\lambda}{4\pi}\right)\int_V \frac{g_1 g_2 \sigma}{(r_1 r_2)^2}\, dV \tag{1.1}$$

where A is factor depending on statistical distribution of signals, P_t is transmitting power, λ is the wavelength, V is the common volume of two antenna beams, σ the scattering cross-section. G_t, G_r are the plane wave gains of the TX/RX antennas. Geometrical parameters for this expression are hard to estimate properly, thus approximate calculation using empirical model is better option. International agreement is on model specified in recommendation of ITU-R P.617-1. Using it we can determine the average annual troposcatter transmission loss prediction for percentages of time between about 50% and 99.9999%. This does not consider antenna loss and absorption in gas molecules. Formulation is following

$$\begin{aligned} L_{617} = M + 30\log f + 30\log\theta_0 + 10\log d + 20\log(5+\gamma H) \\ + 4.34\gamma h_0 + L_c - Y_p \end{aligned} \tag{1.2}$$

where M is atmospheric coefficient in [dB] and γ the atmospheric structure coefficient [km^{-1}]. Aperture-to-medium coupling loss of an antenna is expressed as

$$L_c = 0.07\exp(0.055(G_t + G_r)) \tag{1.3}$$

H denotes the height between the lowest scattering point and the connection between TX/RX antennas

$$H = 10^{-3}\frac{\theta_0 d}{4} \quad [\text{km}] \tag{1.4}$$

h_0 denotes the height between lowest scattering point and ground, a_e is here a median effective earth radius

$$h_0 = 10^{-6}\frac{\theta_0^2 a_e}{8} \quad [\text{km}] \tag{1.5}$$

θ_0 is scatter angle, which can be expressed as through TX/RX horizon angles θ_t, θ_r

$$\theta_0 = 10^3\frac{d}{a_e} + \theta_t + \theta_r \quad [\text{mrad}] \tag{1.6}$$

and Y_p is conversion factor for non-exceedance percentages p other than 50%.[7]

1.2.3 Atmospheric ducting

In particular meteorological conditions may form a layer in troposphere with abnormal refractive index due to a temperature inversion. This layer may formed through various mechanisms. For example when cold air blows over warmer ocean water. If the inversion layer is strong enough, it is capable of reflecting radio waves. Mostly VHF and UHF bands, but in occasionally even HF band. That effect of reflection waves from troposphere back to ground is called surface duct. It enables significantly longer propagation by means of sky wave. Another similar effect is called elevated duct, that is when radio signal is reflected by high layer and then again reflected by layer below, thus it's trapped between two layers and reflects in this "pipe". By this even longer distances may be achieved, but it's rarer condition. In general we see ducting more as a source of interference, because it's too rare for any useful service usage. It only brings far over signals to areas where they're not expected.[5]

1.3 Ionospheric propagation

For understanding of ionospheric scattering, we have to first be acknowledge with structure and properties of ionosphere itself.

1.3.1 Ionosphere

Ionosphere is ionized part of Earth's atmosphere which ranges from about 50km up to 600km altitude. The ionization is a result of solar radiation, which

strips gas molecules of their outer electrons and leaves them positively charged. These gas molecules have tendency to recombine with free electrons. The degree of ionization is thus result of constant impact of opposing processes. As the degree is clearly dependant on solar activity, it's self-evident that there are differences between day time. During day we distinguish 4 layers, D, E, F1 and F2. In night the F layer blend to one called F, the D layer doesn't exist in night due to absence of solar radiation.[6] [5]

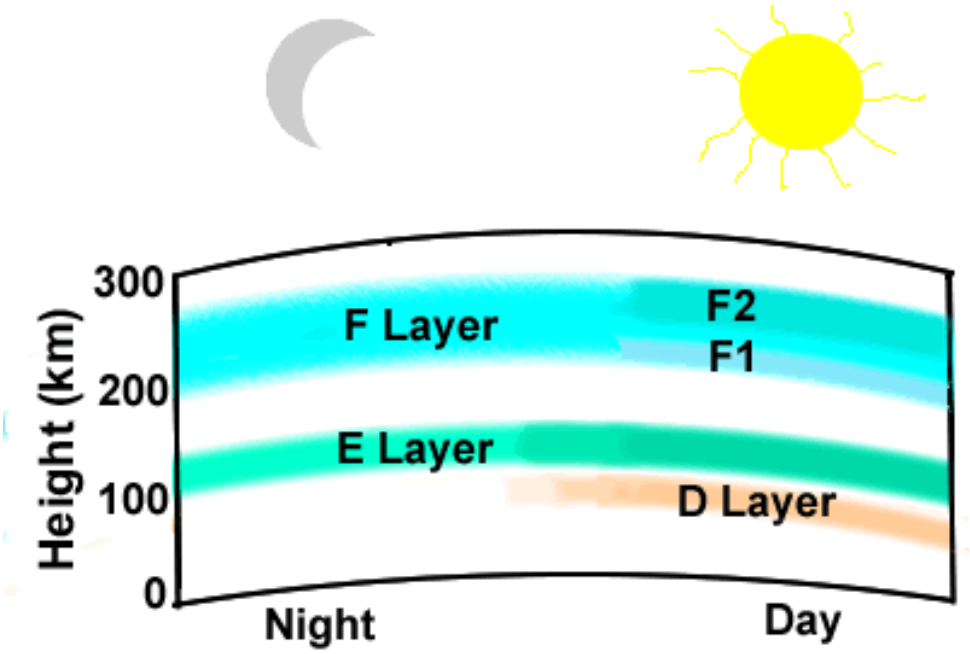

Figure 1.1: Layers of ionosphere [1]

1.3.2 Ionoscatter

Ionosphere can reflect radio waves back to ground in similar way as we discussed in Atmospheric ducting chapter. In contrast to meteorologically set layers in troposphere, in ionosphere the duration and behaviour is more consistent. We can measure electron density of lower side of ionosphere by ionosonde. It works on radar principle, ground station transmits signal vertically and nearby station records it's reflection. From transit time the path length and thus reflection layer height is determined.

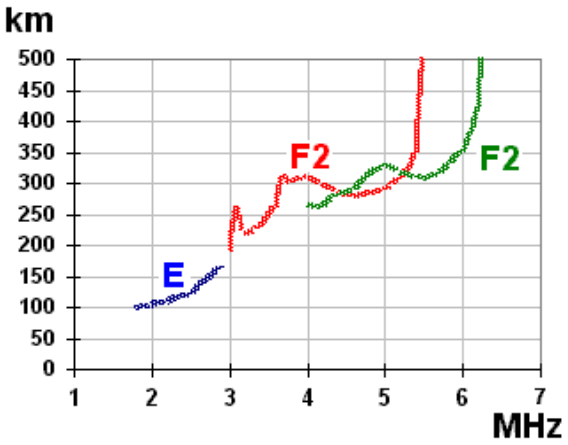

Figure 1.2: Example of ionosonde measurement results [2]

The lowest frequency at which the reflection to ground fails is called critical frequency f_c. Typical range is between 4-12MHz with maximum at noon. If the radio wave is not launched vertically but under certain angle, the path through ionosphere is considerably longer and thus the chance of collision is raising. We then define maximum usable frequency (muf) for communication as

$$f_m = \frac{f_c}{\sin\theta} \tag{1.7}$$

With usage of reflection from F layers, it's possible to reach very long distances. This also means that transmitted signal will be subject to selective fading and severe non-linear distortion in the receiver. Suitable modulation and bandwidth management is necessary for such communication.

1.4 Radio noise

Radio noise is defined by ITU-R as "A time-varying electromagnetic phenomenon having components in the radio-frequency range, apparently not conveying information and which may be superimposed on, or combined with, a wanted signal.". It can be divided into natural noise and man-made noise. For the purpose of this work we'll focus only on radio noise emanating from sources external to the radio receiving system.[3]

1.4.1 Natural noise

Major causes of natural noise are:

- Emissions from atmospheric gases and hydrometeors
- The ground or other obstructions within the antenna beam
- Radiation from celestial radio sources
- Radiation from lightning discharges (atmospheric noise due to lightning)

Emissions from atmospheric gases and hydrometeors are more significant on lower frequencies as in VHF/UHF there are more significant noise sources e.g. Sun. Representational values are stated in following graphs.

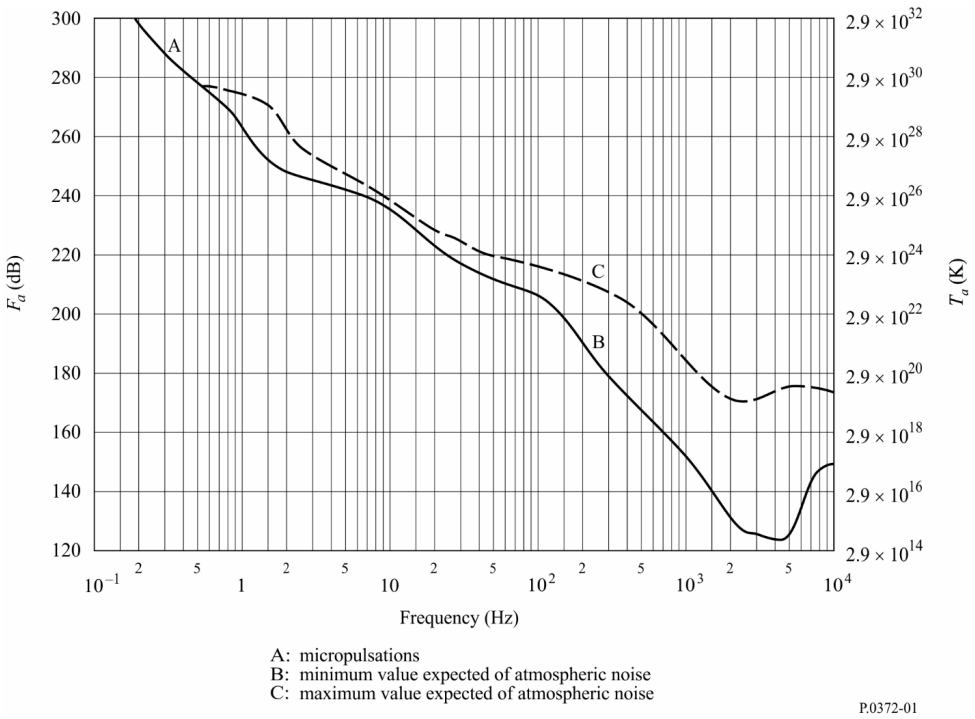

Figure 1.3: F_a versus frequency (10^{-1} to 10^4 Hz) [3]

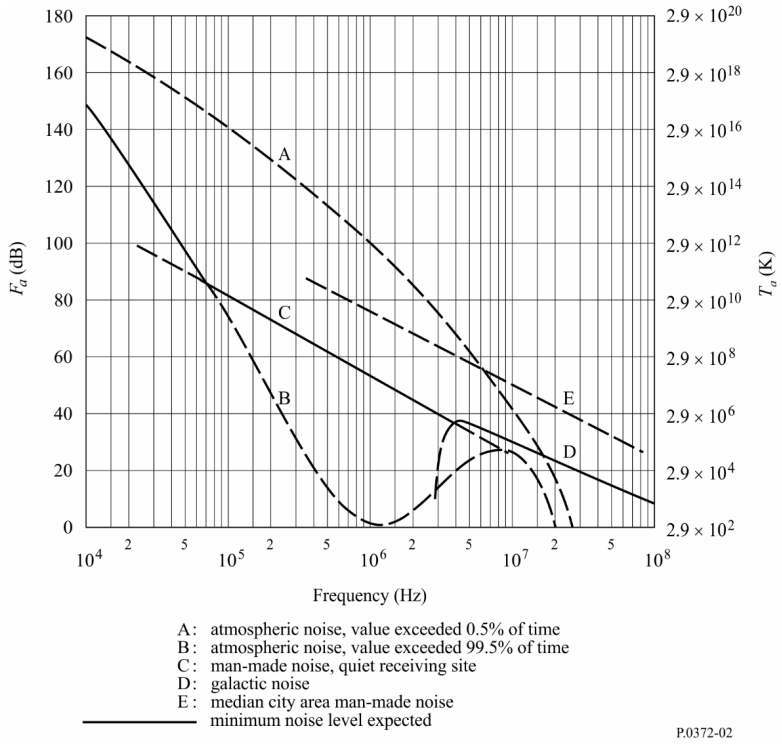

Figure 1.4: F_a versus frequency (10^4 to 10^8 Hz) [3]

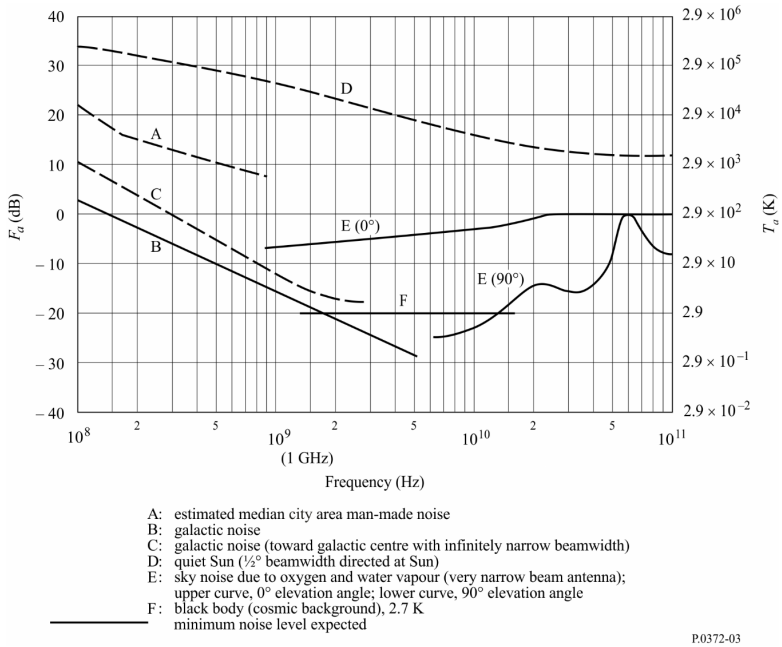

Figure 1.5: F_a versus frequency (10^8 to 10^{11} Hz) [3]

Radiation from celestial radio sources can be split into two groups. One is communications below 2 GHz and second is communications above 2 GHz. Below 2 GHz we need to be concerned with the Sun and the Milky Way galaxy, which appears as a broad belt of strong emission. Galactic noise will not be observed at frequencies lower than the critical frequency of ionospheric F2 layer (foF2), which ranges between 4-12 MHz. Above 2 GHz, we need to consider only the Sun and a few very strong non-thermal sources such as Cassiopeia A, Cygnus A and X and the Crab nebula since the cosmic background contributes 2.7 K only and the Milky Way appears as a narrow zone of somewhat enhanced intensity. The brightness temperature range for the common extra-terrestrial noise sources in the frequency range 0.1 to 100 GHz is illustrated below.

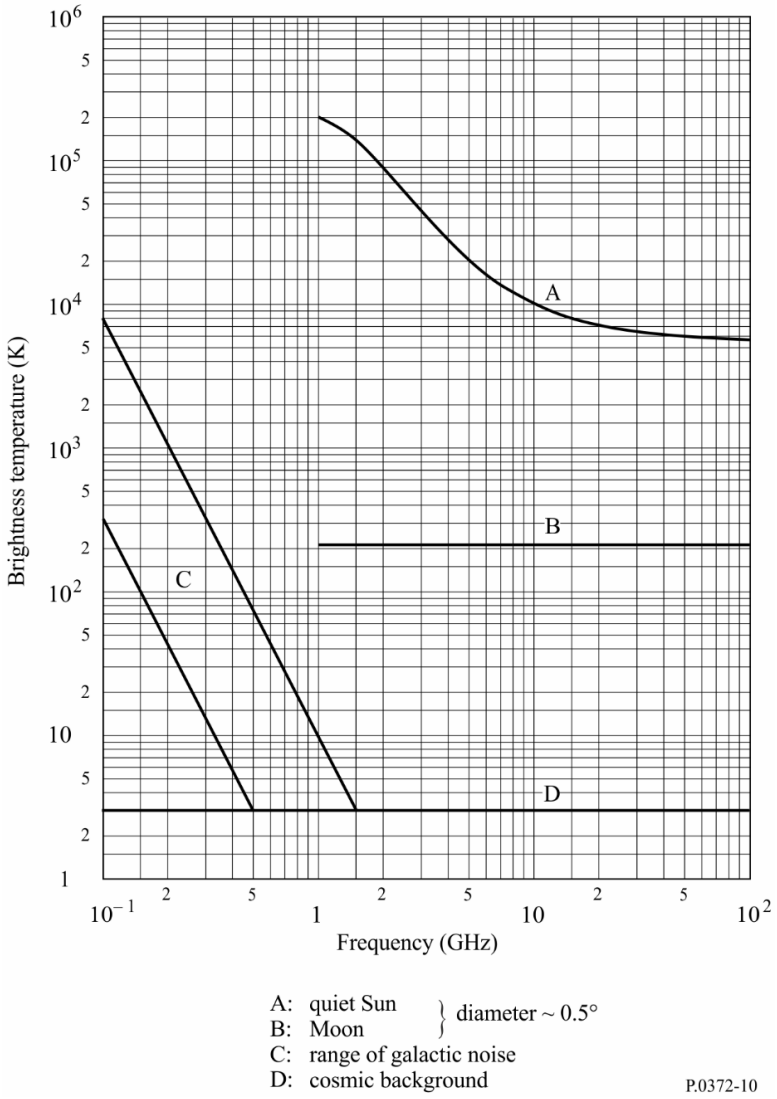

Figure 1.6: Extra-terrestrial noise sources [3]

Radiation from lighting discharges dominates at VLF (very low frequency) and LF (low frequency). On a worldwide scale, 3.5 million lightning flashes occur daily, which are about 40 lightning flashes per second. It can be observed as combination of white noise (coming from distant thunderstorms) and impulse noise (coming from a near thunderstorm). Form of radio energy that lighting stroke has is called whistler and is characterized by a whistling tone of decreasing pitch that may last for several seconds.[1]

1.4.2 Man-made noise

Man-made noise is particularly generated by various outdoor antennas. Aggregated unintended radiation from electrical machinery, equipment and power transmission lines is also significant. Often man-made noise has impulsive components, which may impact radio systems. This is heavily dependent on real location.

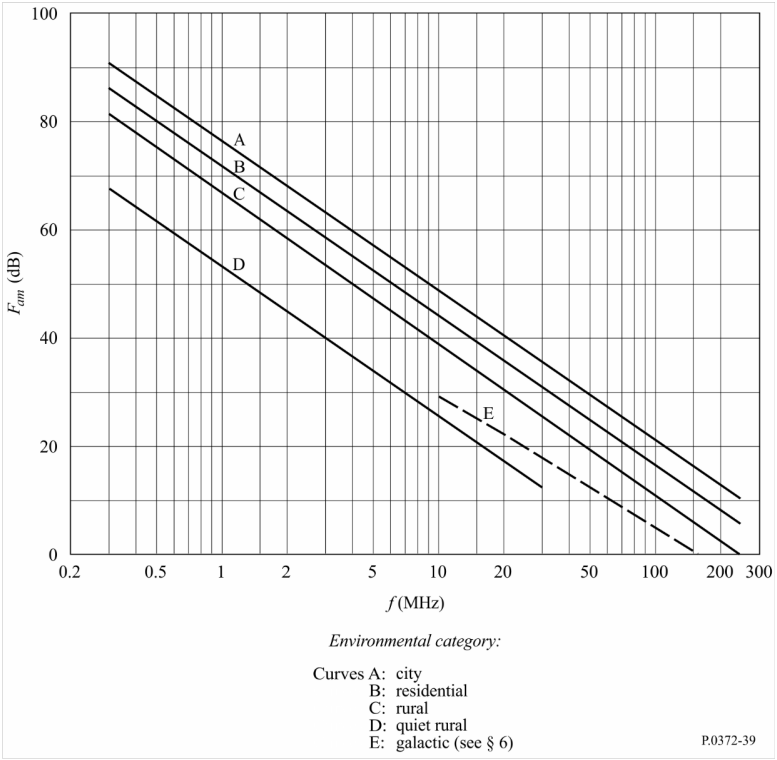

Figure 1.7: Median values of man-made noise power for a short vertical lossless grounded monopole antenna [3]

[1] Due to specific display of lightning stroke in frequency domain and long distance propagation on VLF and LF, it can be observed from long distance. With several observer stations exact location can by obtained. This lead to development of project Blitzortung, which is real time map of lightning strokes all around the world. www.blitzortung.org

1.5 Low-Density-Parity-Check codes

Low-Density-Parity-Check (LDPC) codes were designed by Robert Gray Gallager in his Sc.D. thesis in 1960 and published in 1963. For years they went relatively unnoticed as their computational complexity is rather high. Currently are LDPC codes considered as a best option for high code rates e.g. 1/2, 2/3, 4/5, and 7/8. They're specified by sparse matrix with very high dimensionality, thus code words are also of very high dimensionality. We can divide them into two groups. Regular codes, where number of ones in each row and column is fixed and irregular codes, where the number varies.[9] Encoder for LDPC can be build in several ways. Straightforward way is to obtain generator matrix G be inverting parity check matrix H. Then encoder can be simple matrix multiplication.[10]

$$\mathbf{c} = G\mathbf{d} \tag{1.8}$$

where $\mathbf{c}$ is codeword and $\mathbf{d}$ is data word. This way has several issues. First, for rather dense G the encoding complexity is quadratic in the codeword length. Second, requirements as $n - k$ variable nodes have degree ≤ 2 comes at price of decoding threshold and minimum distance.[10]

1.6 JT9 protocol

JT9 communication protocol was created for amateur radio purposes by Joseph Hooton Taylor Jr. (K1JT). It is designed for making minimum valid QSOs, that is connection where both sides exchanges their IDs and possibly signal report, at LF,MF and HF under extreme weak-signal conditions. JT9 uses strong convolutional code with rate $r = 1/2$ and constraint length $K = 32$ and very narrow bandwidth 9-FSK modulation.[11]

1.6.1 Encoding process

13 characters message is source encoded using 42 characters alphabet (10 numbers 0 - 9, 26 upper case letters A-Z, 6 punctuation symbols [space] + - . / ?) into 13 numbers $c_n = 0 - 41$. Then they're formed into 3 numbers of

length 27, 27 and 17 bits as follows.

$$\begin{aligned} N_1 &= \Big(\big((c_1 \cdot 42 + c_2) \cdot 42 + c_3\big) \cdot 42 + c_4\Big) \cdot 42 + c_5 \\ N_2 &= \Big(\big((c_6 \cdot 42 + c_7) \cdot 42 + c_8\big) \cdot 42 + c_9\Big) \cdot 42 + c_{10} \\ N_3 &= (c_{11} \cdot 42 + c_{12}) \cdot 42 + c_{13} \end{aligned} \tag{1.9}$$

After that N_{1-3} are rearranged to be more contiguous and one bit is added to determine format of message, because JT9 can either transmit structured message or plain text. Setting bit 15 of N_3 to 1 marks plain text message.

$$\begin{aligned} N_1 &= 2N_1 + \left(\left(\frac{N_3}{2^{15}}\right) \bmod 2\right) \\ N_2 &= 2N_2 + \left(\left(\frac{N_3}{2^{16}}\right) \bmod 2\right) \\ N_3 &= (N_3 \bmod 2^{15}) + 2^{15} \end{aligned} \tag{1.10}$$

N_{1-3} are now 28, 28 and 16 bits long. We combine them into sequence.

$$2^{(16+28)}N_1 + 2^{16}N_2 + N_3 \tag{1.11}$$

With padding 31 zeros at the end we obtain 103 bit long sequence. Convolutional codding with rate 1/2 and constraint length 32 is applied. Rate $r = 1/2$ appends two bits to output for each input bit. Added bits serve as a forward error correction (FEC). Constraint length $K = 32$ states window length from which parity bit is calculated. Exact structure of convolutional coder is specified by two 32 bit long numbers, which represents polynomials of order 31. JT9 uses 0xF2D05351 and 0xE4613C47. 206 bits from convolutional coder are interleaved so the adjacent bits are dispersed in sequence. Interference occurs mostly in bursts, by interleaving the resistance against interference is raised. Channel symbols are formed by combining triplets of bits, for that we pad one zero at the end to have number of bits divisible by 3. We obtain 69 channel symbols with values 0-7. We further encode them using Gray code in which each successive symbols differs in one bit. This helps minimize significance of errors from noise or distortion. Synchronization is ensured by inserting 16 zeros amongst 69 data symbols as specified by synchronisation vector S.

$$\begin{aligned} S = {} & 11001000010000010000001000000 \\ & 00010100000000000000001100100 \\ & 00100000100000010000000000101 \end{aligned} \tag{1.12}$$

Ones represents inserted zeros, zeros represents positions for data symbols. Values of data symbols are shifted by adding one from 0-7 to 1-8. Obtained $69 + 16 = 85$ symbols with values 0-8 are modulated with 9-FSK modulation. Sampling frequency is 12kHz, symbol rate is 1.736 baud, tone spacing is 1.736Hz which gives total bandwidth $9 \times 1.736 = 15.624$Hz.[11]

Chapter 2

Channel models

Radio wave propagation is dependant on many variables as frequency, distance, polarization modes, terrain, scattering, reflecting and many more. Covering all of that with one model is simply not possible. It is clear that each model will have some advantage and be more specialized.

2.1 Fading channels

Fading channels as their name states are designed to model fading phenomena. It's variation of attenuation of a signal with some variable, for example with prolong distance, or with complexity of terrain, which may introduce multipath propagation. We can divide them into two types, large scale fading and small scale fading.[8]

2.1.1 Large-scale fading

Large-scale fading, as name hints, models significant attenuation, large obstacles and losses over prolong paths. First of such models is *Free space path loss model*. It's used to forecast received signal strength in line-of-sight (LOS) environment. As it doesn't count with any obstacles between transmitter and receiver, it's usage is limited and mostly serves for satellite communication

calculations. We can write the received power $P_r(d)$ as

$$P_r(d) = \frac{P_t\, G_t\, G_r\, \lambda^2}{(4\pi)^2\, d^2\, L} \tag{2.1}$$

d is distance between transmitter and receiver, P_t is transmitted power, G_t and G_r are TX/RX antenna gains, λ is wavelength. In terrestrial environment reducing of power with logarithmic way is more accurate. Thus *Log distance path loss model* is simple but usable model that includes path fading by introducing n index, that represents environment.

$$PL_{LD}(d)[dB] = PL_F(d_0) + 10n\, \log_{10}\left(\frac{d}{d_0}\right) \tag{2.2}$$

d_0 is reference distance.
Hata model match description of various environments including cities, suburbs and also open area. It's based on Okumura model, but uses correction factor $a(h_r)$ to adapt for each environment. For small-medium cities it's

$$a(h_r) = (1.1 \log_{10}(f_c) - 0.7)h_r - (1.56 \log_{10}(f_c) - 0.8)\ [dB] \tag{2.3}$$

For larger cities when $f_c \geq 300$MHz, it's

$$a(h_r) = 3.2(\log_{10}(11.75h_r)^2 - 4.97\ [dB] \tag{2.4}$$

Equation for Hata model in urban area is following[8]

$$\begin{aligned} P_{L,urban}(d)\ [dB] =& 69.55 + 26.16 \log_{10}(f_c) - 13.82 \log_{10}(h_t) \\ & - a(h_r) + (44.9 - 6.55 \log_{10}(h_t) \log_{10}(d)) \end{aligned} \tag{2.5}$$

2.1.2 Small-scale fading

Small-scale fading is for rather close range communication, where constructive/destructive interference due to multiple paths lead to rapid fluctuations in signal level.
Rayleigh fading is the simplest probability model of the taps of channel filters. It's based on assumptions, that there exist many statistically independent paths of scattering and that these paths are random in corresponding to the amplitude of the delay window. The phase of i-th path is $2\pi f_c \tau$. If we take d_i as the propagation distance of i-th path, and λ as a wavelength assuming $d_i \gg \lambda$. Thus we can assume that phase is uniformly distributed in range $0 - 2\pi$. Each path tapping is

$$h_i[m] = a_i(m/W) \exp^{-j2\pi f_c \tau_i (m/W)} \operatorname{sinc}[1 - \tau_i(m/W)W] \tag{2.6}$$

That can be modelled as a cyclic symmetry complex random variable. We assume variance of $h_l[m]$ is function of tapping, however, not correlated with time variable m. Thus the probability density is

$$|h_l[m]| = \frac{x}{\sigma_l^2} \exp\left(\frac{-x^2}{2\sigma_l^2}\right) \quad x \geq 0 \tag{2.7}$$

Rician fading has also many independent paths, known amplitude and lots of components in line-of-sight (LOS). It can be modelled as follows if it satisfy condition $|h_l[m]| \geq l$ [8]

$$h_l[m] = \sqrt{\frac{\kappa}{\kappa+1}}\,\sigma_l \exp^{j\theta} + \sqrt{\frac{1}{\kappa+1}}\,CN(0,\sigma_l^2) \tag{2.8}$$

Chapter 3

Experimental part

First we replicate JT9 protocol in Matlab and verify it's functionality by local transmission. For verification of correct encoding and decoding we use software WSJT-X, which can decode JT9 protocol transmission from WAV audio file. Next we build in Matlab modified version with channel encoding using LDPC code and verify it by local and long distance transmission. All source codes are attached to electronic version and on physical medium with printed version.

3.1 Replication of JT9 protocol

3.1.1 Encoding process

Encoding process of JT9 protocol was implemented in Matlab straightforward as described in theoretical part. Input is 13 characters long massage, output is audio file, which can be easily used as input for radio transmitter. Messages for encoding were of 3 types as stated in Table 3.1. Message number 1 was chosen as a uncommon form for JT9. Number 2 has valid call sign in first half and random second half. Number 3 has same first half and valid grid identification in second. As we proceed according encoding process we obtain channel symbols. We modulate them using 9-FSK modulation on a carrier frequency $F_c = 1\text{kHz}$, which was chosen as a comfortable value in audio range.

Message number	Content
1	A1B2 .?C3D4E5
2	OK1FLZ ABCDEF
3	OK1FLZ JN79IA

Table 3.1: Encoded message types.

3.1.2 Decoding process

Input for decoding process is audio file with same properties as output in encoding process. First we need to demodulate and detect channel symbols. For that simple demodulation was implemented. For duration of each channel symbol the power spectrum is calculated. Then frequency of power peak is taken as the most probably transmitted frequency. Value of channel symbol is determined by subtracting carrier frequency and dividing by frequency separation value. Removing synchronization symbols, Gray decoding, channel symbol to bit sequence conversion and deinterleaving is same as in encoding part, just done inversely. Obtained bit sequence was decoded using Fano algorithm, which principle is described below. Following procedures are again inverse to those in encoding part and thus message is decoded into text.

3.1.3 Fano algorithm

Fano algorithm is sequential decoding algorithm. It uses rather intuitive method for searching of suitable way in coder tree. It works on a one path at the time, moving forward along the path. At each node it calculates metrics increments for every way from the node, choosing the most probable (highest metric increment), but only if it exceeds initially chosen threshold value. If not, the threshold is lowered by constant and forward nodes are reexamined. If metrics still doesn't exceed threshold, algorithms moves backwards and chooses another node to move forward. If the node was already the least probable, it'd lead to cycle, so for such a case threshold would be lowered again. Due to limited number of explored paths, the result of Fano algorithm may be different from most probable path obtained by Viterbi algorithm. However, with 2^K branches for each message bit, Fano algorithm is much less memory demanding.[12]

3.2 Modified variation of JT9 protocol

Modification of JT9 was performed mainly in replacing convolutional code with very long constraint length, which is demanding on computational time at both encoding and decoding, with LDPC code. Code design is above scope of this work, thus existent (174,91) LDPC code design was chosen from protocol FT8. It's specified by generator matrix with dimensions 83×91. For codeword verification serve the sparse parity check matrix of dimensions 83×174. To integrate the code, changes were made to length of bit sequence entering channel encoding.[13]

3.2.1 Encoding process

13 characters long message is source encoded and bit sequence is formed same way as in JT9, just number of padded zeros is reduced to 19. Sequence of 91bits is encoded with LDPC code into 174bits. These are formed into $174/3 = 58$ symbols, which are then Gray encoded. Synchronization is done by inserting specific sequence of channel symbols in the beginning, middle and ending of transmission, thus from 58 symbols we obtain 79 channel symbols. Used modulation is 8-FSK, which is less exotic than 9-FSK as typical size of alphabet is in powers of 2. Carrier frequency remains the same as in out implementation of JT9, but bandwidth is widen to $8 \times 6.25 = 50$Hz, which allows us to raise equally symbol rate to 6.25 baud. Raised-cosine function is used for shaping beginning and ending of each channel symbol waveform. Output is audio signal in WAV format. [13]

3.2.2 Decoding process

Decoding process is same as for our JT9 implementation. With only differences in adaptation to slightly changed modulation and LDPC decoding instead of Fano algorithm.

3.3 Experimental transmission

All transmissions were conducted in similar way. Audio files were played on laptop with audio output directed to Microham USB Interface III. That enables control of transceiver YEASU FT-950 via CAT interface. It also serves as DA converter for analog input of transceiver, which we used here. Transceiver YEASU FT-950 mixes this analog input with set carrier frequency and pass it to antenna. Maximum power output is 100W, but antenna accessories is not suitable for more than 20W. As a receiver for local transmissions was used hand-held AOR AR8200D, with frequency range 100kHz to 3GHz and analog audio output. For recording from the audio output we used PC audio input and WSJT-X software, because it can record directly from audio driver with sampling frequency we require.

Figure 3.1: Transceiver workplace

3.3.1 JT9 local transmission

Transceiver minimal power output is 5W, which would saturate input of our receiver if not attenuated. For that we used 50Ω impedance load instead of antenna, imperfection of it leads to very weak radiating. This was then possible to received and record. Transmission was conducted on frequency 50MHz (6m band). Decoding into message was performed by `JT9_decode_local.m`. Bit errors are displayed in figure below. We can see that errors from transmission were all repaired by convolutional coding. Message was acquired without errors.

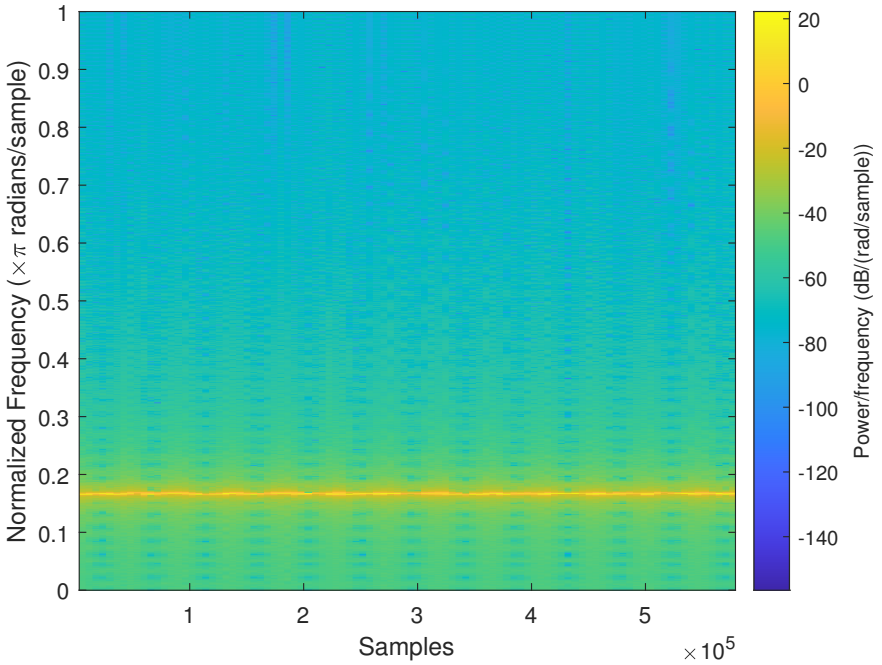

Figure 3.2: Spectrogram of received signal, locally transmitted by our implementation of JT9

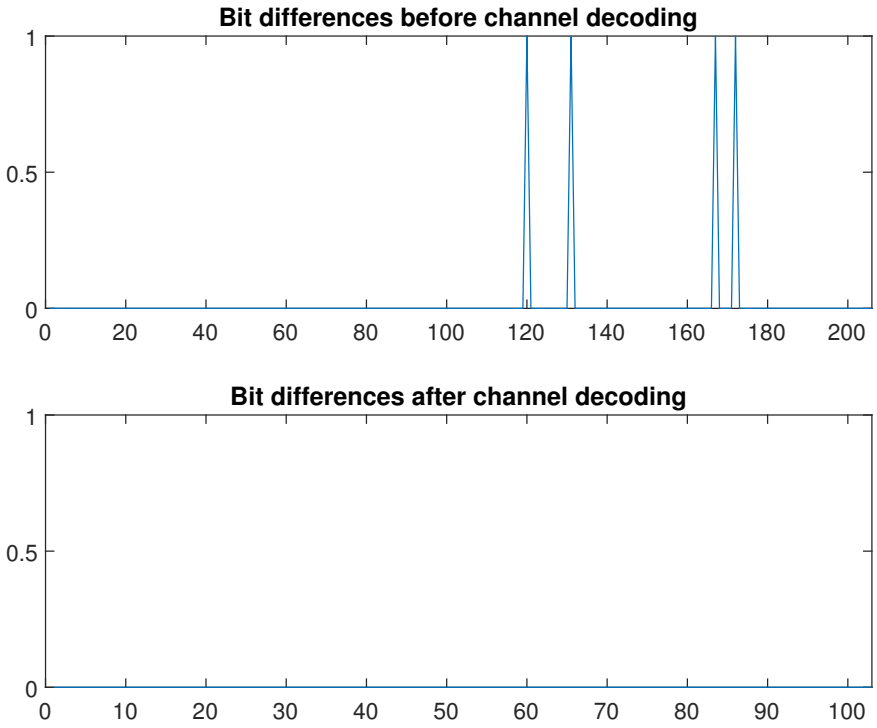

Figure 3.3: Comparison of pre-decoded and post-decoded bit sequence errors

3.3.2 Modified JT9 local transmission

Conducted same way as a previously described transmission. Decoding into message was performed by `LDPC_decode_local.m`. Bit errors are displayed in figure below. Errors from transmission weren't repaired, but as they're in area of zero padding, they're not affecting transmitted data and thus message was acquired without errors.

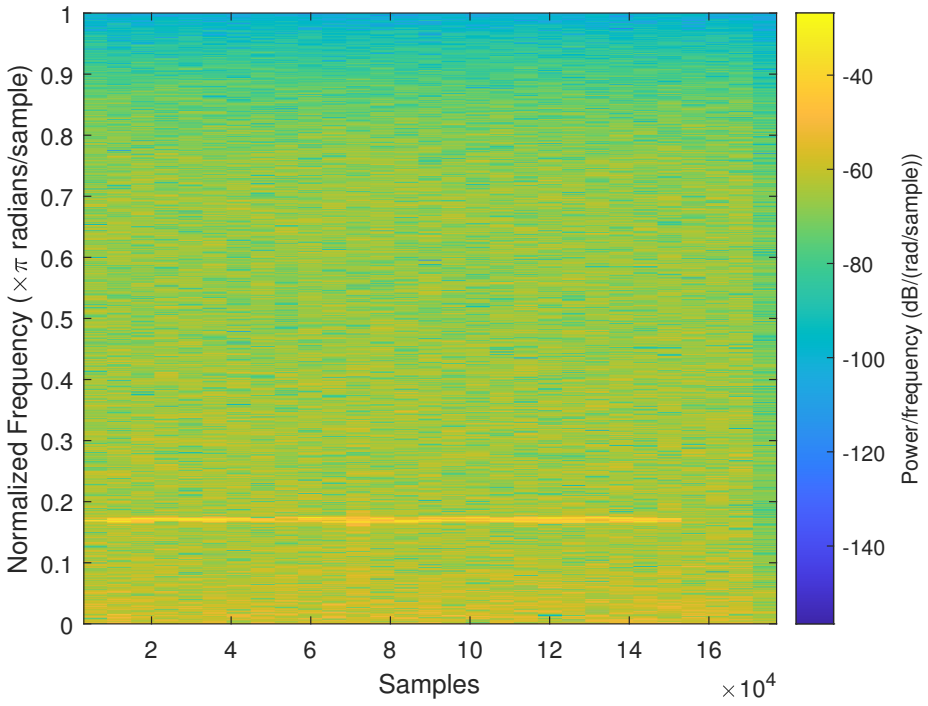

Figure 3.4: Spectrogram of received signal, locally transmitted by our implementation of modified JT9

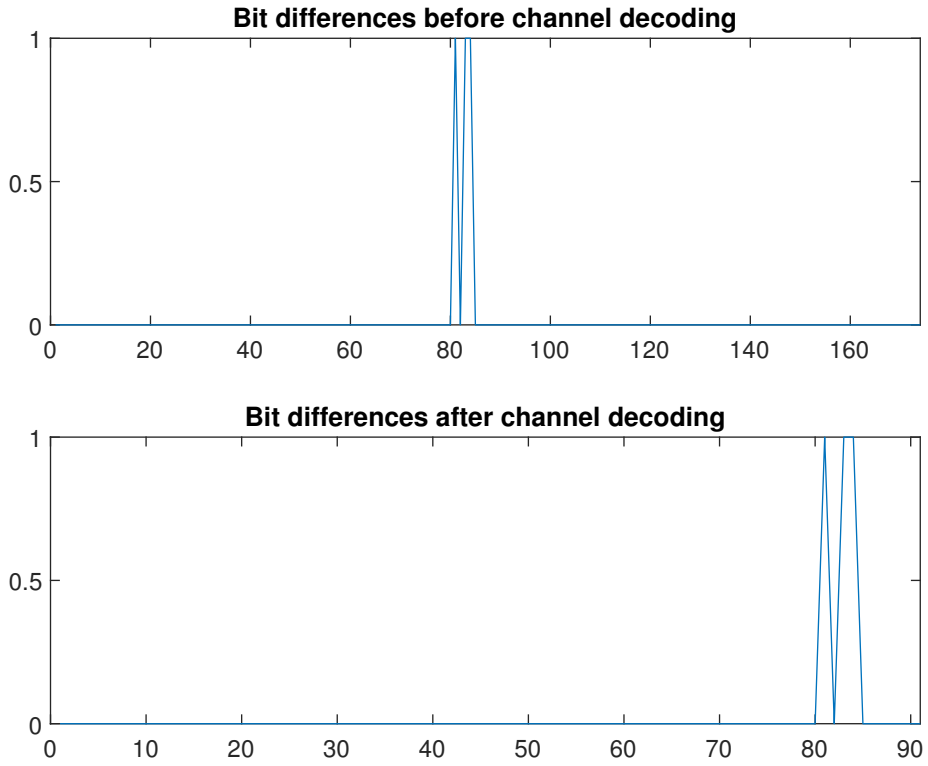

Figure 3.5: Comparison of pre-decoded and post-decoded bit sequence errors

3.3.3 Modified JT9 remote transmission

Remote transmission was conducted with higher power of 20W and half wave vertical antenna. Chosen frequency was 28MHz as atmosphere conditions were more suitable for this band. For receiving was used online SDR (software defined radio) receiver located in Floriac(Bordeaux, France), which can be remotely operated through web browser.[1] It's equipped with antenna "GP 27 Venom 1/2", which is also half wave vertical. SDR technology allows simultaneous usage for several users, as each can tune it independently. Recording of audio output is performed through build-in function.
Decoding of this signal was more difficult as such a long distance impacts spectral properties of signal. Detected carrier frequency was shifted against transmitted by 71.9Hz, probably due to Doppler spread of the channel. It could also be due to error in receiver, however that can't be verified as we don't have direct access to it. Detected bit sequence was errorless, decoding introduce one error in output sequence. However, it is na area of padded zeros and thus doesn't affect data transmission. Message was acquired without errors.

[1] More similar receivers are listed at http://www.websdr.org/

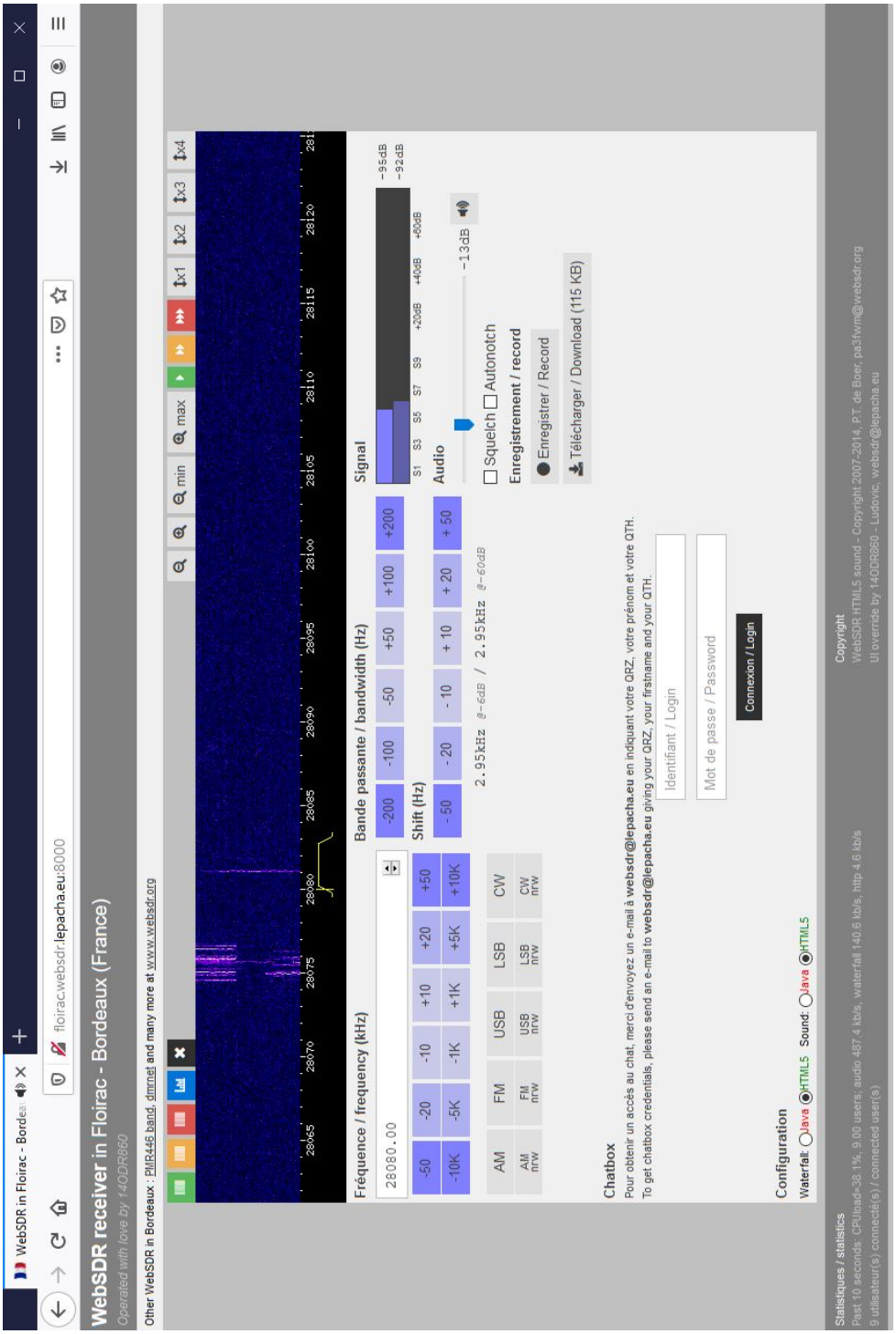

Figure 3.6: WebSDR interface

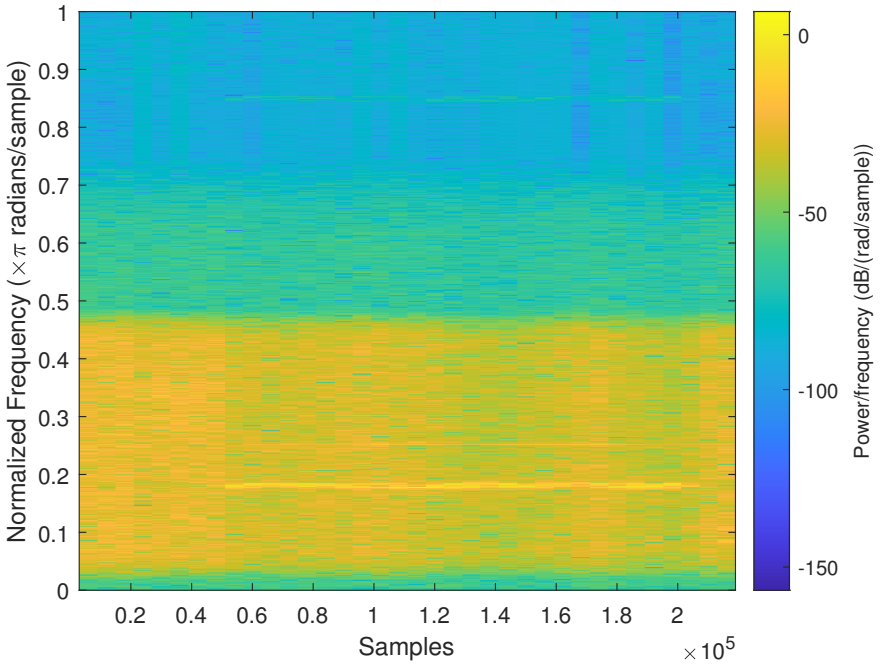

Figure 3.7: Spectrogram of received signal, transmitted to remote receiver located in France by our implementation of modified JT9

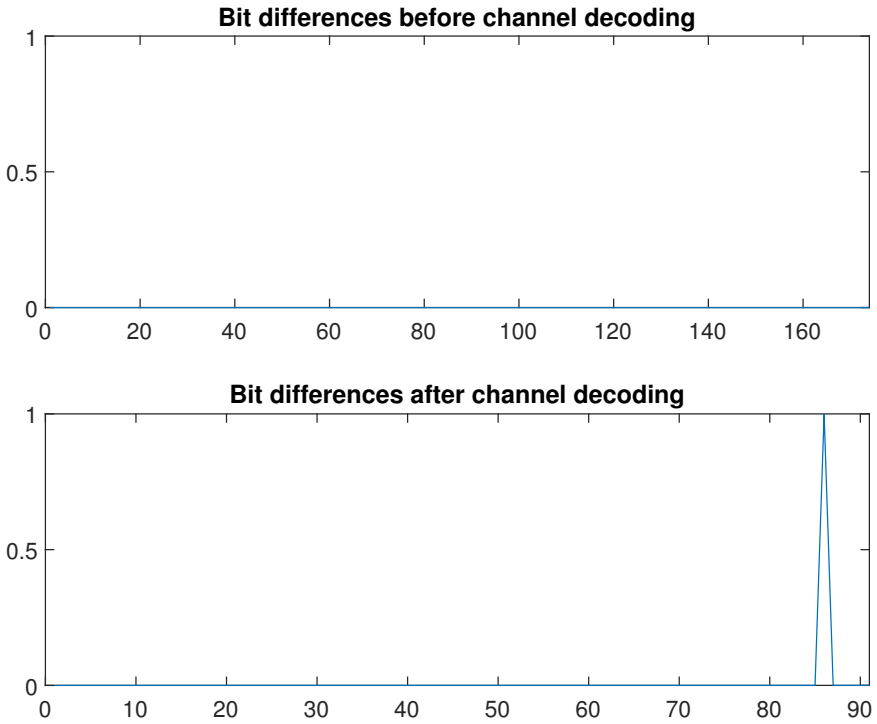

Figure 3.8: Comparison of pre-decoded and post-decoded bit sequence errors

Figure 3.9: Half wave vertical antenna used for remote transmission

3.4 Proposition of measurement method

In this section we'll discussed proposition of measurement method for broadband troposcatter/ionoscatter channel properties. Our intention is to bring some insight to channel properties. As we introduced in first chapter, both troposcatter and ionoscatter may at good condition reflect rather vertical radio wave back to ground and thus allows us to reach further distances than with ground wave. These condition are ceaselessly changing. Appreciable effort is made for their measurement and prediction. Interesting idea was presented in article "Determination of the ionospheric foF2 using a stand-alone GPS receiver"[14], where using double-tuner GPS receiver and numerical plasma model input were researches able to determine foF2 of ionosphere in near-real-time. Using such measurement of ionosphere for channel estimation and improving transmit characteristic is possible way.
Other may be long term monitoring of for example continuous transmitting of predetermined message. Such process would need to be as much stand-alone as possible to provide sufficiently long monitored time. In remote transmission described above could be both sides of TX/RX controlled by one person. However, as it was transmission on a frequency not intended for public use, it could only be operated by person with proper certification according Czech law regulation 156/2009 Sb. That had to be kept in mind for other such experiments.
About technical design of possible experiment. Modification of JT9 made in this thesis would be sufficient starting point.

Chapter 4

Conclusion

Both JT9 and its modified version were successfully transmitted and decoded. Possible measurement method were discussed above. Regarding future work, if modified JT9 should be used, the decoder needs to be improve. Currently it's working good enough, but I'd considered it as the weakest part regarding error probability. As for transmitted amount of useful data, there's also room for improvement as it wasn't the goal of this work.

Appendix A

Content of CD

CD
- Long-Distance Digital Troposcatter and Ionoscatter Radio Communication in HF VHF UHF band.pdf
- JT9_decode.m
- JT9_decode_local.m
- JT9_encode.m
- JT9_local.wav
- LDPC_decode.m
- LDPC_decode_local.m
- LDPC_decode_websdr_france.m
- LDPC_encode.m
- LDPC_local.wav
- LDPC_WebSDR_France.wav
- LDPCparity.mat
- mettab.dat
- partab.dat

Appendix B

Bibliography

[1] Layers of ionosphere, wikipedia, upload.wikimedia.org/wikipedia/commons/7/7e/ionosphere_layers_en.svg.

[2] Example of ionosode measurements results, wikipedia, upload.wikimedia.org/wikipedia/commons/6/69/ionogramme.png.

[3] Radiocommunication Sector. Recommendation itu-r p.372-14 radio noise. Technical report, International Telecommunication Union, 2019.

[4] Joseph Henderson Reynolds. Understanding troposcatter propagation. Master's thesis, United States Air Force Academy, 1982.

[5] *Radio Antennas and Propagation*. Newnes, 1998.

[6] *Radio Propagation and Adaptive Antennas for Wireless Communication Links*. John Wiley & Sons, Inc., 2007.

[7] L. Li, Z. Wu, L. Lin, R. Zhang, and Z. Zhao. Study on the prediction of troposcatter transmission loss. *IEEE Transactions on Antennas and Propagation*, 64(3):1071–1079, 2016.

[8] Jing Gong Yiwang Huang Huajun Chen, Lina Yuan. Various channel models in wireless communication. In *2017 International Conference on Computer Systems, Electronics and Control (ICCSEC)*.

[9] Robert G. Gallager. *Low-Density Parity-Check Codes*. PhD thesis, Cambridge, 1963.

[10] Sam Dolinar Jon Hamkins Christopher R. Jones Kenneth S. Andrews, Dariush Divsalar and Fabrizio Pollara. The development of turbo and ldpc codes for deep-space applications. *Proceedings of the IEEE*, 2007.

[11] *WSJT-X 2.2 User Guide, www.physics.princeton.edu/pulsar/K1JT/wsjtx-doc/wsjtx-main-2.2.2.html.*

[12] R. N. Piplia Anup Dey Kapil Gupta, P. K. Ghosh. A comparative study of viterbi and fano decoding algorithm for convolution codes. *AIP publishing*, 2010.

[13] Bill Somerville G4WJS Joe Taylor K1JT Steve Franke, K9AN. The ft4 and ft8 communication protocols. *QEX*, 2020.

[14] Christina Oikonomou Wedyanto Kuntjoro Dudy D. Wijaya, Haris Haralambous. Determination of the ionospheric fof2 using a stand-alone gps receiver. *Springer*, 2017.

BACHELOR'S THESIS ASSIGNMENT

I. Personal and study details

Student's name: **Horáček Jakub** Personal ID number: **465990**

Faculty / Institute: **Faculty of Electrical Engineering**

Department / Institute: **Department of Radioelectronics**

Study program: **Open Electronic Systems**

II. Bachelor's thesis details

Bachelor's thesis title in English:

Long-Distance Digital Troposcatter and Ionoscatter Radio Communication in HF/VHF/UHF band

Bachelor's thesis title in Czech:

Long-Distance Digital Troposcatter and Ionoscatter Radio Communication in HF/VHF/UHF band

Guidelines:

Student will first get acquainted with fundamentals of radio communications using troposcatter (TS) and ionoscatter (IS) channel. It should involve a deep survey of available channel models and power budget measurements. Student should also get acquainted with advanced modulation and coding suitable for these ultra hight attenuation scenarios (eg. coded CPM, LDPC codes, etc.). The goal of the work is two-fold. (1) Student should build a simple narrowband digital communication PHY layer modulation and coding processing (e.g. with parameters similar to JT9 system) for TS (IS) channel and practically verify its functionality using analog TxR frontend. (2) Student should develop estimation and measurement methods that could bring some insight in broadband TS/IS channel properties and possibilities of using advanced wideband waveforms, processing (e.g. equalization) and coding methods. A suitable long distance experimental link should be setup for work goal (1) and optionally for (2). The work should include a practical implementation of remote access of the far-end of the experimental link (e.g. over the internet) that would allow to conduct the long-distance experiments.

Bibliography / sources:

[1] IEEE papers on TS/IS propagation (ieeexplore.ieee.org)
[2] Proakis: Digital communications, McGraw Hill 2001

Name and workplace of bachelor's thesis supervisor:

prof. Ing. Jan Sýkora, CSc., Department of Radioelectronics, FEE

Name and workplace of second bachelor's thesis supervisor or consultant:

Date of bachelor's thesis assignment: **03.02.2020** Deadline for bachelor thesis submission: **14.08.2020**

Assignment valid until: **30.09.2021**

prof. Ing. Jan Sýkora, CSc. Supervisor's signature	doc. Ing. Josef Dobeš, CSc. Head of department's signature	prof. Mgr. Petr Páta, Ph.D. Dean's signature

III. Assignment receipt

The student acknowledges that the bachelor's thesis is an individual work. The student must produce his thesis without the assistance of others, with the exception of provided consultations. Within the bachelor's thesis, the author must state the names of consultants and include a list of references.

Date of assignment receipt	Student's signature